Flow Characteristic and Trapping Characteristics of Cycloid Rotor Pump

Ren Zhenxing, Liu Chunyan and Li Yulong

Flow Characteristic and Trapping Characteristics of Cycloid Rotor Pump

Ren Zhenxing[1]，Liu Chunyan[2]，Li Yulong[1]

1.*Industrial Manufacturing School, Chengdu University, Chengdu, Sichuan 610106, China ；*

2. *Safety, Environment & Technology Supervision Research Institute, PetroChina Southwest Oil & Gasfield Company，*

Chengdu, Sichuan 610041, China ；

Abstract: To accurately calculating the flow rate of cycloid rotary pump, as well as to correctly understand its trapped oil phenomenon. Firstly, the instantaneous flow rate formula of cycloid rotary pump was established based on the method of swept area, and compared with the two present approximate formulas by an example.Secondly, based on the just established flow rate formula and the created trapped oil model in present literature, the trapped oil pressure of a single cavity near in the minimum volume position was simulated. It is pointed that for cycloid rotary pump by an example, the flow non-uniform coefficient is 6.45%, in contrast, the flow nonuniformity coefficient of external gear pump is 21.2%; Relative to the accurate results, the two present approximate errors of flow rates are 1.93% and 2.90%; and the present approximate error of flow non-uniform coefficient is 7.13%; when the minimum position angle is added by 0.5° or 1° or 2°, relative to discharge pressure of the pump, the corresponding maximum peak of trapped oil pressure is increased by 1.6% or 6.0% or 21.7%. The results indicate that the flow characteristics of cycloid rotary pump is better than external gear pump; the two present approximate errors of flow rate are little,but the present approximate error of flow non-uniform coefficient is higher; also there is a trapped oil phenomenon in cycloid rotary pump,but not obvious.

Key words: cycloid rotary pump， flow characteristics，trapped oil characteristics， simulation， trapped oil model，swept area， trapped oil pressure

As an internal cycloid gear pump ("cycloid rotor pump" for short) having a mesh with tooth difference, its characteristics are to take the equidistant curve of complete curtate epicycloid as the inner rotor tooth profile, and the outer rotor tooth profile is circular arc profile conjugated with it. The pump is widely used in the various hydraulic systems, including the vehicles [1], because it has such advantages as compact size, simple structure, stable operation, small noise and good high-speed performance. In the recent decades, a lot of studies are carried out on it at home and abroad. In the Literature [2], the tooth profile envelope forming method of the cycloid pump is studied on the basis of the envelope theory in the differential geometry; in the Literature [3], the production method of cyclical toothing and spiral rotor and their geometry are studied with the gear pump and the cycloidal toothing on the Roots blower; in the Literature [4], the geometric correction method of the cycloidal profile is proposed; in the Literature [5-11], the study is carried out on the curve and the formation of its envelope line with the principle of gear meshing and differential geometry theory from different aspects, the foreign scholars mainly focus on studying the meshing theory of tooth profile, and there are relatively few studies on the actual application problem; and in the Literature [12-15], the study is carried out on the determination of the meshing clearance and its tooth profile design and influence of pressure distribution. The domestic literatures are mainly reflected in the study and design of tooth profile [1, 16-18] and parameter selection and optimization [19-21]. In the Literature [1], the detailed study and simulation calculation are carried out on the pump theory; and in the Literature [21], the volume of its working cavity is calculated and analyzed, but the computational process is too complicated, therefore, the practicability is not strong. Since the tooth form of the inner and outer rotors is relatively complicated, there are not many studies on the flow (displacement) characteristics of the pump currently, and in the actual application, the approximation formula is mostly used for calculating [22]. For the trapping phenomenon, it is thought that the trapping phenomenon is not presented by the internal meshing pump in the common sense, but the trapping phenomenon of the internal gear pump is studied and described in the literatures and part of network data [23]. In view of this, the paper plans to carry out the further study on the flow characteristics and trapping characteristics of the pump, so as to hope to get the accurate flow calculation formula, and correctly understand the trapping phenomenon of the pump.

1. Flow Characteristics

In Fig.1, it describes three positions of the cycloid rotor pump in a complete oil absorption process. In Fig.1a, it indicates the minimum volume position of a working cavity, called minimum position for short; in Fig.1c, it indicates the maximum volume position of a working

cavity, called maximum position for short; and in Fig.1b, it indicates one unspecific volume position of a working cavity between the maximum and minimum, called one unspecific position for short. The formed meshing points of a working cavity are set as n_1 and n_2 respectively, the volume is set as V_1, the inner rotor is called the wheel o_1 for short, and the outer rotor is called the wheel o_2 for short, wherein the wheel o_1 and the wheel o_2 refer to the corresponding wheel center.

In Fig.1b, the angle that the wheel o1 and o2 turn is set as $d\varphi_1$ and $d\varphi_2$ in the small time dt. At this time, the small variation dV_1 of V_1 is

$$dV_1 = 0.5b(r_{11}^2 - r_{21}^2)d\varphi_1 + 0.5b(r_{12}^2 - r_{22}^2)d\varphi_2 \quad (1)$$

In the formula, r_{11} and r_{12} indicate the distance from the point n_1 to the wheel center o_1 and o_2; r_{21} and r_{22} indicate the distance from n_2 to o_1 and o_2; b indicates the tooth width; and φ_1 and φ_2 indicate the included angle between x_1 axis and x_2 axis of the dynamic coordinate $x_1 o_1\ y_1$ and $x_2 o_2\ y_2$ of the wheel o_1 and o_2 and the x axis of the fixed coordinate system $x o_2 y$ respectively, namely, the rotation angle of the wheel o_1 and o_2. When $\varphi_2 = 0$, x_1 axis and x_2 axis is coincided with the x axis.

In Fig.1b, if the drop foot of n_1 and n_2 on the center line $o_1 o_2$ is set as k_1 and k_2, it exists in the right triangle $\triangle o2\ n_1 k_1$ and $\triangle p n_1 k_1$

$$r_{11}^2 - (r_1 - k_{p1})^2 = l_1^2 = f_1^2 - k_{p1}^2 \quad (2)$$

In the formula, r_1 indicates the pitch radius of o_1; f_1 and k_{p1} indicate the length from the node p to the point n_1 and point k_1; and l_1 indicates the length from n_1 to k_1. Similarly,

$$\left. \begin{array}{l} r_{12}^2 - (r_2 - k_{p1})^2 = l_1^2 = f_1^2 - k_{p1}^2 \\ r_{21}^2 - (r_1 - k_{p2})^2 = l_2^2 = f_2^2 - k_{p2}^2 \\ r_{22}^2 - (r_2 - k_{p2})^2 = l_2^2 = f_2^2 - k_{p2}^2 \end{array} \right\} \quad (3)$$

In the formula, r_2 indicates the pitch radius of o_2; f_2 and k_{p2} indicate the length from the point p to the point n_2 and point k_2; and l_2 indicates the length from n_2 to k_2.

z_1 and z_2 are set as the tooth number of the gear o_1 and o_2; i is set as the transmission ratio; ω_1 and ω_2 are set as the angular speed of the wheel o_1 and o_2, therefore, for the cycloid rotor pump, it has:

$$i = z_1/z_2 = r_1/r_2 = d\varphi_2/d\varphi_1 = \varphi_2/\varphi_1 = \omega_2/\omega_1 \quad (4)$$

By substituting the Formula (2)-(4) into the Formula (1), the change rate DV_1 of V_1 to time can be derived as follows

$$DV_1(\varphi_2) = dV_1/dt = 0.5(1-i)\omega_1 b \left[f_1^2(\varphi_2) - f_2^2(\varphi_2) \right] \quad (5)$$

In Fig.1b, c_1 and c_2 indicate the center of circle of two adjacent formed generating circles of V1. Since $\angle c_1 o_2 c_2 = 2\pi/z_2$, $\angle c_2 o_2 x = \varphi_2 - 2\pi/z_2$. Therefore, in the triangle $\triangle o_2 c_1 p$ and $\triangle o_2 c_2 p$, it has

$$\left. \begin{array}{l} f_1(\varphi_2) = \sqrt{L^2 + r_2^2 - 2Lr_2\cos\varphi_2} - R \\ f_2(\varphi_2) = f_1(\varphi_2 - 2\pi/z_2) \end{array} \right\} \quad (6)$$

In the formula, L indicates the radius of the generating circle; and R indicates the radius of the enveloping circle.

If $\varphi_2 = \pi/z_2$ in Fig.1a and $\varphi_2 = \pi + \pi/z_2$ in Fig.1c, the total output flow Qsh of the pump is the sum of all positive or negative DV_1 in a circle according to the volume of z_2 single working cavities in a circle that the wheel o_2 rotates, namely

$$Q_{sh}(\varphi_2) = \sum_{j=1}^{z_2} DV_1 \left[\varphi_2 - (j-1)2\pi/z_2 \right] \quad (DV_1 \geq 0) \quad (7)$$

a.最小位置　　　　　　　　　　　b.某一位置　　　　　　　　　　　c.最大位置

a. The minimum position　　　b. A certain position　　　c. The maximum position

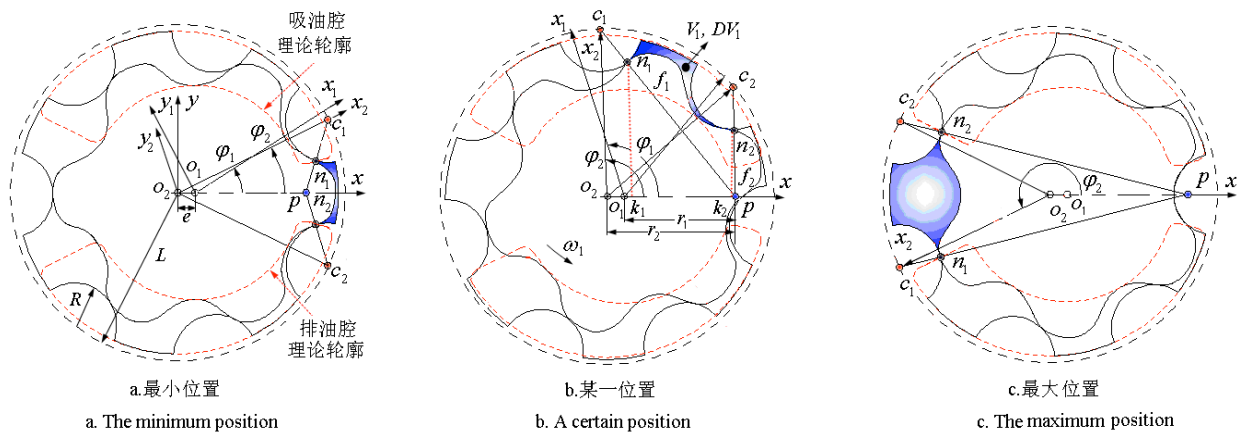Fig.1 Minimum volume and maximum volume and one unspecific position of a working cavity

2. Instance Analysis of Flow Characteristics

The center distance, i.e. e=2.5*10^{-3} m, z_1=6, z_2=7, R=8.8×10^{-3} m, L=24.5×10^{-3} m, b=20×10^{-3} m, is used; the speed of the wheel o_1 is 2000 r/min, and its geometric calculation shall be shown in the Literature [19]. The

corresponding DV_1 and Q_{sh} under the above parameters shall be shown in Fig.2a-b. It can be seen from Fig.2 that, DV_1 (shown in the small circle 1 in Figure) near the minimum position is gentle, relative to that (shown in the small circle 2 in Figure) near the maximum position. It can be seen from Fig.2b that, the maximum flow is 3.293×10^{-4} m^3/s, the minimum flow is 3.085×10^{-4} m^3/s, and the average flow is 3.226×10^{-4} m^3/s, so the

nonuniform coefficient of the flow is δ=(3.293−3.085)/3.226=6.45%, which is much more stable than the nonuniform coefficient of 21.2% flow for the external gear pump with the tooth number of 10 [22], and the pulse frequency $_Q$=n_2z_2/60 of the flow is consistent with that of the external gear pump which is provided with the side clearance [22], wherein n_2 indicates the speed of the wheel o_2.

The approximate calculation formula of the two flows given in the Literature [22] and their nonuniform coefficient is as follows:

$$Q_{s1} = 0.5\omega_1 b(r_{a1}^2 - r_{f1}^2)$$
$$Q_{s2} = 0.5\omega_1 b r_{f2}^2 [0.5687 - 0.0333(L-R)/e] \quad (8)$$
$$\delta_s = [16.5 - 2.36(L-R)/e + 0.44L/e]\%$$

a. 单工作腔容积变化率
a. The changed rate of working volume

b. 瞬时流量
b. The instantaneous flow rate
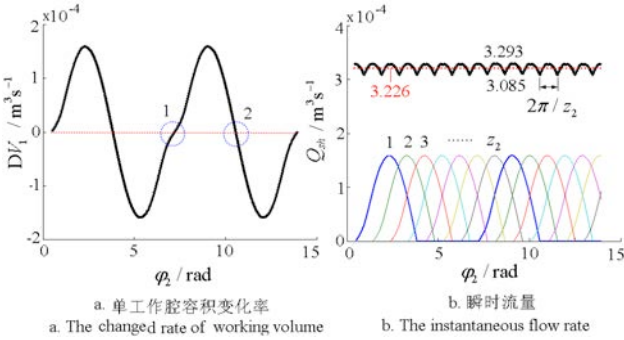
Fig.2 Changed volume rate of a working cavity and total instantaneous flow

After the calculation, Q_{s1}= 3.288*10^{-4} m^3/s; Q_{s2}= 3.227*10^{-4} m^3/s; and δ_s= 5.99%. Two approximation errors of the flow are 1.93% and 2.90% respectively; and the approximation error of the nonuniform coefficient of the flow is 7.13%, wherein the approximation error of the flow is relatively small, and the approximation error of the nonuniform coefficient of the flow is on the high side.

3. Trapping Characteristics

3.1 Trapping model

The working pressure of oil in V_1 is set as p_1, and if the volume increase of V1 is positive, it is obtained as followed according to the definition of the elasticity modulus of the fluid [24-27].

$$dp_1/dt = K_1[-DV_1 - Q_n(p_1) - Q_o(p_1) - Q_r(p_1)]/V_1 \quad (9)$$

In the formula, K_1 indicates the bulk modulus of the oil; Q_n indicates the exchange flow that the inside and outside of V_1 pass through the meshing clearance at the point n_1 and n_2; Q_o indicates the exchange flow that the inside and outside of V_1 pass through the axial clearance of the end face; and Q_r indicates the exchange flow between V_1 and outside oil absorption cavity and oil drainage cavity. And −DV_1 is marked as the trapped oil flow.

The theoretical crescent oil absorption cavity and oil drainage cavity of the pump can be opened into the form shown in Fig.1 and Fig.3, and the oil absorption cavity and oil drainage cavity are arranged symmetrically. The included angle of the oil cavity with x axis in the minimum position is set as γ_i, and called the included

angle of the oil cavity in the minimum position for short; and its included angle with -x axis in the maximum position is set as γ_o, and called the included angle of the oil cavity in the maximum position for short. But in fact, the density of the sealing area between the oil absorption cavity and oil drainage cavity is often increased at the oil absorption site by improving ⊿γ_i value appropriately on the basis of γ_i, so as to improve the volumetric efficiency [1]; and meanwhile, the sufficient oil absorption is often reached at the oil absorption side with the flow inertia of the oil by reducing ⊿γ_o value appropriately on the basis of γ_o, so as to improve the volumetric efficiency [1]. In order to facilitate the characteristic analysis of the trapped oil, the actual oil absorption cavity and oil drainage cavity are arranged symmetrically, as shown in Fig.3.
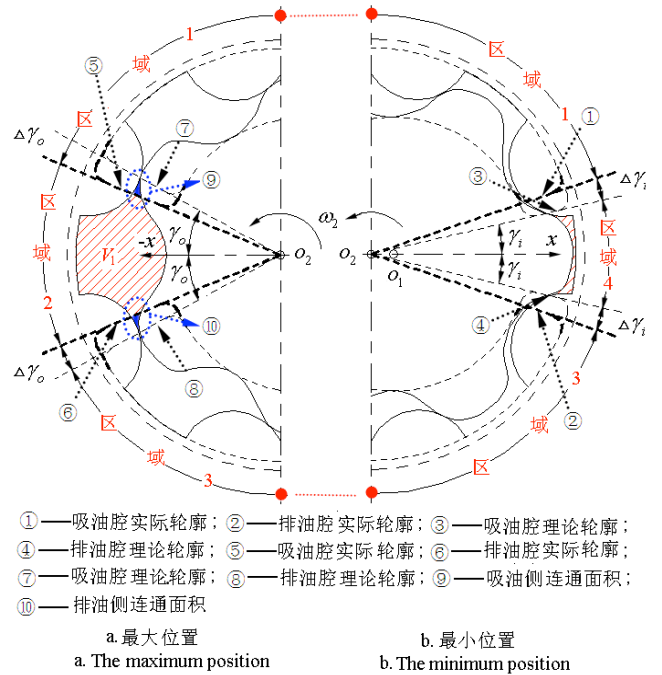

① ——吸油腔实际轮廓；② ——排油腔实际轮廓；③ ——吸油腔理论轮廓；
④ ——排油腔理论轮廓；⑤ ——吸油腔实际轮廓；⑥ ——排油腔实际轮廓；
⑦ ——吸油腔理论轮廓；⑧ ——排油腔理论轮廓；⑨ ——吸油侧连通面积；
⑩ —— 排油侧连通面积

a.最大位置
a. The maximum position

b. 最小位置
b. The minimum position

Fig.3 Theory outline and actual contour in the maximum and minimum volume position

-吸油腔实际轮廓	Actual contour of oil absorption cavity
排油腔理论轮廓	Actual contour of oil drainage cavity
吸油腔理论轮廓	Theoretic contour of oil absorption cavity
排油腔理论轮廓	Theoretic contour of oil drainage cavity
-吸油腔实际轮廓	Actual contour of oil absorption cavity
排油腔实际轮廓	Actual contour of oil drainage cavity
吸油腔理论轮廓	Theoretic contour of oil absorption cavity
排油腔理论轮廓	Theoretic contour of oil drainage cavity
吸油侧连通面积	Connected area of oil absorption side
排油侧连通面积	Connected area of oil drainage side
区域1	Area 1
区域2	Area 2

	Area 3

In Fig.3, when the wheel o2 rotates a circle, V1 goes through the following four areas. Area 1: $[\gamma_i + \triangle\gamma_i, \pi-\gamma_o+\triangle\gamma_o]$, area 2: $[\pi-\gamma_o+\triangle\gamma_o, \pi+\gamma_o-\triangle\gamma_o]$, area 3: $[\pi+\gamma_o-\triangle\gamma_o, 2\pi-\gamma_i-\triangle\gamma_i]$, and area 4: $[2\pi-\gamma_i-\triangle\gamma_i, 2\pi+\gamma_i+\triangle\gamma_i]$. V_1 in area 1 is always contacted with the oil absorption cavity fully, and V_1 in area 2 is a little big relative to the trapped oil flow near the minimum position, but V_1 is always contacted with the oil absorption cavity and oil drainage cavity fully, as shown in the connected area of the oil absorption and oil drainage sides in Fig.3a; and V_1 in area 3 is always contacted with the oil drainage cavity fully. Therefore, $Q_r \approx -DV_1$ in the three areas, so, the obvious trapping phenomenon will not be presented, and we will not analyze it too much here. But, V_1 in area 4 is small, relative to the trapped oil flow near the maximum position, but V_1 is always not contacted with the oil absorption cavity and oil drainage cavity, namely, $Q_r=0$, and the probability of the obvious trapping phenomenon is relatively big, therefore, we focus on the analysis of trapping characteristics in this area. So, the Formula (9) is simplified into

$$dp_1 / d\varphi_2 = K_1[-DV_1 - Q_n(p_1) - Q_o(p_1)]/(\omega_2 V_1) \qquad (10)$$

3.2 Leakage rate

In consideration of machining error and processing cost in the actual production, the meshing clearance of radial tooth top is often taken $h_n = 0.02*10^{-3}$ m-$0.10*10^{-3}$ m [1], and the axial clearance of the end face is often taken ho=$0.02*10^{-3}$ m-$0.12*10^{-3}$ m [1].

In Fig.1 and Fig.3, the wheel o_1 is taken as the drive wheel, the power shall be transmitted by the meshing point located at one side of the oil absorption cavity, so as to push the driven wheel o_2 to rotate, therefore, the clearance at these meshing points can be approximate to 0; but the power cannot be transmitted at the meshing point locates at one side of the oil drainage cavity, therefore, the clearance at these meshing points can be approximate to h_n [11-14]. Therefore, the meshing points at one side of the oil drainage cavity are not the meshing points in the true sense, and here, we define them as the side clearance points; the clearance here is defined as the gear side clearance; and the exchange flow Q_n passing through the gear side clearance at the point n_1 and n_2 is called the side clearance flow for short. The meshing point n_1 in Fig.3 is located at one side of the oil absorption cavity, and the meshing point n_2 is located at one side of the oil drainage cavity. So [24]

$$Q_n(p_1) = sign(p_1 - p_o)C_n b h_n \sqrt{2|p_1 - p_o|/\rho} \qquad (11)$$

In the formula, sign () indicates to take the positive and negative signs in the bracket, and its value is -1 when being negative and 1 when being positive; p_o indicates the oil drainage pressure of the pump; ρ indicates the density of the working oil; and C_n indicates the flow coefficient of the thin-walled hole.

In Fig.4a, the axial leakage arisen from the peripheral closed outline of V_1 is mainly composed of four parts respectively [28], i.e. quantity Q_{o1} of leakage ① flowing to o_1 and o_2 axis, quantity Q_{o2} of leakage ② flowing to the oil drainage cavity, quantity Q_{o3} of leakage ③ flowing to the oil absorption cavity, and quantity Q_{o4} of leakage ④ flowing to the outer ring of the wheel o_2; and the above-mentioned leakage rate is positive for outflow. The path length of the leakage ① is far more than that of leakage ②~④, so the leakage ① can be ignored, namely, $Q_o = Q_{o2} + Q_{o3} + Q_{o4}$.

In Fig.4a, the included angle of arc section g_1g_2 of the tooth space of the wheel o_2 corresponding to the center of the circle of the axis o_2 is

$$\alpha_{f2} = 2\pi / z_2 - 2a\cos\left[(L^2 + r_{f2}^2 - R^2)/(2Lr_{f2})\right] \qquad (12)$$

In the formula, r_{f2} indicates the root radius of o_2; and based on the flow formulate of long and thin hole, Q_{o4} is obtained as follows:

$$Q_{o4} = \frac{\alpha_{f2}r_{f2}h_o^3}{12\mu(r_{D2} - r_{f2})}(p_1 - p_i) \qquad (13)$$

In the formula, μ indicates the viscosity of the oil; and r_{D2} indicates the radius of the outer ring of the wheel o_2.

In Fig.4a, the leakage path of ② and ③ can be approximate to the trapezoid path shown in Fig.4b when the pump is rotated in area 4. So [28]

$$\left.\begin{array}{l} Q_{o2}(\varphi_2) = \dfrac{h_2 h_o^3 \ln(b_2 / a_2)}{12\mu(b_2 - a_2)}(p_1 - p_o) \\[3mm] Q_{o3}(\varphi_2) = \dfrac{h_3 h_o^3 \ln(b_3 / a_3)}{12\mu(b_3 - a_3)}(p_1 - p_i) \end{array}\right\} \qquad (14)$$

In the formula, p_i indicates the oil absorption pressure of the pump.

In Fig.4a, the point n_2 located on the actual contour line of the oil drainage cavity is taken as the initial position of trapping analysis and the included angle of n_2 to the initial position is set as α_{2n}, so

$$\left.\begin{array}{l} a_2 = r_{22}\sin\alpha_{2n}\ ;\ \ b_2 = r_{f2}\sin(\alpha_{2n} + \gamma_i - 0.5\alpha_{f2}) \\ h_2 = r_{f2}\cos(\alpha_{2n} + \gamma_i - 0.5\alpha_{f2}) - r_{22}\cos\alpha_{2n} \\ a_3 = r_{12}\sin(2V\gamma_i - \alpha_{2n})\ ;\ b_3 = r_{f2}\sin(\gamma_i + 2V\gamma_i - 0.5\alpha_{f2} - \alpha_{2n}) \\ h_3 = r_{f2}\cos(\gamma_i + 2V\gamma_i - 0.5\alpha_{f2} - \alpha_{2n}) - r_{22}\cos(2\gamma_i + 2V\gamma_i - \alpha_{2n}) \end{array}\right\} (15)$$

In $\triangle n_2c_2o_2$, set $\angle n_2c_2o_2 = \theta_2$, rad; and in $\triangle n_1c_1o_2$, set $\angle n_1c_1o_2 = \theta_1$, rad, so

$$\left.\begin{array}{l} r_{12}(\varphi_2) = \sqrt{L^2 + R^2 - 2LR\cos\theta_1} \\ r_{22}(\varphi_2) = \sqrt{L^2 + R^2 - 2LR\cos\theta_2} \end{array}\right\} \qquad (16)$$

Wherein, in $\triangle c_1o_2p$ and $\triangle c_2o_2p$, it can obtain the following formula according to the geometrical relationship of triangle:

$$\left.\begin{array}{l} r_2\sin(\pi - \theta_1 - \varphi_2) = L\sin\theta_1 \\ r_2\sin[\pi - \theta_2 - (\varphi_2 - 2\pi/z_2)] = L\sin\theta_2 \end{array}\right\} \qquad (17)$$

In $\triangle n_2o_2p$, set $\angle n_2o_2p = \alpha_2$, so

$$\alpha_{2n}(\varphi_2) = \gamma_i + \nabla\gamma_i - \alpha_2(\varphi_2) \tag{18}$$

And, in $\triangle n_2 o_2 p$,

$$\alpha_2(\varphi_2) = a\cos\left[r_{22}^2(\varphi_2) + r_2^2 - f_2^2(\varphi_2)\right]/\left[2r_{22}(\varphi_2)r_2\right] \tag{19}$$

In Fig.3b, if the corner deviation of theoretical and actual contour at two sides of the oil absorption cavity and oil drainage cavity relative to the wheel o_2 is set as $\Delta\varphi_2$, namely, the value range of φ_2 is $[\pi/z_2 - \Delta\varphi_2, \pi/z_2 + \Delta\varphi_2]$. So, $\varphi_2 = \pi/z_2$ is substituted into the Formula (19), and at this time, α_2 is equal to γ_i; and $\varphi_2 = \pi/z_2 - \Delta\varphi_2$ is substituted into the Formula (19), and at this time, α_2 is equal to $\gamma_i + \Delta\gamma_i$, namely

$$\gamma_i = \alpha_2(\pi/z_2) \quad ; \quad \Delta\gamma_i = \alpha_2(\pi/z_2 - \Delta\varphi_2) - \gamma_i \tag{20}$$
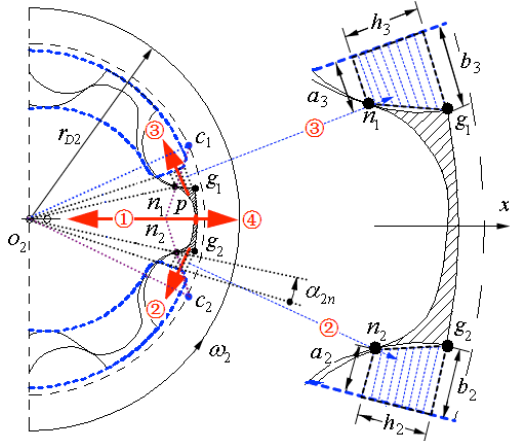
a.轴向泄漏　　　　　b.放大图(3.2:1)
a. Axial leakage　　　b. Local amplification (3.2:1)

Fig.4 Axial leakage paths near in the minimum volume position

4. Instance Analysis of Trapping Characteristics

Based on the relevant parameters in Part 2, the calculation by taking $r_{D2} = 1.5r_{f2}$, r_{f2} again shall be shown in the Literature [1, 19]; and the speed of the wheel o_1 is taken for 5000 r/min, $p_i = 1*10^5$ Pa; $p_o = 10*10^5$ Pa, $h_o = 0.03 \times 10^{-3}$ m; $h_n = 0.03 \times 10^{-3}$ m, $\mu = 0.09$ Pa.s, $C_n = 0.62$, $K_1 = 1.7 \times 10^9$ Pa, $\rho = 870$ Kg/m^3. The trapping model shown in the Formula (10) is subjected to the simulation calculation with Runge-Kutta method [24], and the iterations N are taken for 50000. So the trapped oil pressure corresponding to $\Delta\varphi_2 = 0.5°$, $1°$ and $2°$ and various flows corresponding to $\Delta\varphi_2 = 1°$ are shown in Fig.5.
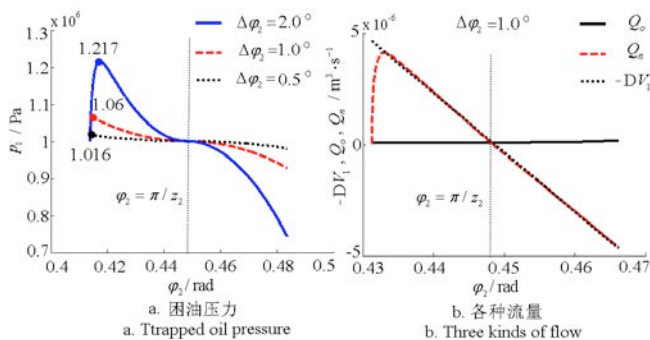

a. 困油压力　　　　　b. 各种流量
a. Ttrapped oil pressure　b. Three kinds of flow

Fig.5 Trapped oil pressure and all flows in the position of minimum volume

In Fig.5a, when $\Delta\varphi_2$ is changed from 0.5° to 1°, until to 2°, the maximum peak of the trapped oil pressure is changed from $1.016*10^6$ Pa to $1.06*10^6$ Pa, until to $1.217*10^6$ Pa, the trapping phenomenon is gradually obvious, and the pressure peak is 1.6%, 6.0% and 21.7% respectively, relative to the increase percentage of the outlet pressure.

In Fig.5b, the trapped oil flow $-DV_1$ is mainly relieved by the side clearance flow Q_n, namely, $Q_n \approx -DV_1$, therefore, the gear side clearance shall be reduced as far as possible. The axial flow is $Q_o << Q_n$, namely, $Q_o \approx 0$. Thus, it can also get the simplest trapping model

$$\frac{dp_1}{d\varphi_2} = \frac{K_1}{\omega_2 V_1}\left[-DV_1(\varphi_2) - Q_n(p_1, \varphi_2)\right] \tag{21}$$

5. Conclusion

1) Under the parameters of the case, the nonuniform coefficient of 6.45% flow of the cycloid rotor pump is much better than that of 21.2% flow of the external gear pump with the tooth number of 10, and the pulse frequency of the flow is consistent with that of the external gear pump which is provided with the side clearance. It can be seen that the flow characteristics of the cycloid rotor pump is far better than that of the external gear pump.

2) Under the parameters of the case, the calculation error of the two approximation formulas for the flow calculation is 1.93% and 2.90% respectively; the approximation error of the nonuniform coefficient of the flow is 7.13%, and the approximation error of the flow is relatively small and conforms to the actual requirement of the engineering, but the approximation error of the nonuniform coefficient of the flow is on the high side; and relative to the external gear pump, the trapping phenomenon is also presented by the cycloid rotor pump, but is not obvious.

3) In practice, it is theoretically practicable to improve the volumetric efficiency by increasing the included position of the oil cavity in the minimum position and decreasing the included angle of the oil cavity in the maximum position.

4) The relatively big side clearance leakage is presented by the rotor pump, therefore, the meshing clearance value of the radial tooth top shall be reduced as far as possible; and the axial leakage is far less than the side clearance leakage, therefore, the axial clearance value can be increased appropriately due to the process demand.

References：

[1] Xu Xuezhong. The internal meshing cycloid gear pump theory research and simulation[D]. Nanjing ： Southeast University，2005．

[2] Vecchiato D.，Demenego A，A rgyris J，et al．Geometry of

a Cycloidal Pump[J]．Computer Methods in Applied Mechanics and Engineering，2001，190(18)：2309－2330.

[3] Litvin F L，Feng Pinghao．Computerized design and generation of cycloidal gearings[J]. Mech. Mach. Theory，1996，31(7)：891－911.

[4] Demenego Alberto，Vecchiato Daniele，Litvin Faydor L．Design and simulation of meshing of a cycloidal pump[J]. Mech. Mach. Theory，2002，37(3)：311－332.

[5] Mimmi G. C., Pennacchi P. E. Non-undercutting conditions in internal gears[J]. Mech. Mach. Theory，2000，35(4)：477－490.

[6] Lee, S. C.．Profile design of the inner rotor of a gerotor by the composite curve of circular arcs[J]．Journal of the KSTLE，2006，22(2)：79–86.

[7] Hsieh, C. F.，Hwang, J. H.．Geometric design for a gerotor pump with high area efficiency[J]．ASME J. Mech. Des., 2007，129(12): 1269–1277.

[8] Hsieh, C. F.．Influence of gerotor performance in varied geometrical design parameters[J]．ASME J. Mech. Des., 2009，131(12)：121008.

[9] G. S. Lee，S. Y. Jung，J. H. Bae，et al．Design of rotor for internal gear pump using cycloid and circular-arc curves[J]．Journal of Mechanical Design，2012，134(1)：011005-1－011005-12

[10] Y Inaguma．Friction torque characteristics of an internal gear pump[J]．Proceedings of the Institution of Mechanical Engineers，Part C: Journal of Mechanical Engineering Science，2011，225(6)：1523－1534.

[11] Chang, Y. J.，Kim, J. H.，Jeon, C. H.，et al．Development of an integrated system for the automated design of a gerotor oil pump[J]．ASME J. Mech. Des.，2012，129(10)：1099–1105.

[12] B Paffoni, R Progri and R Gras．Teeth clearance effects upon pressure and film thickness in a trochoidal hydrostatic gear pump [J]．Proceedings of the Institution of Mechanical Engineers，Part G: J. Aerospace Engineering，2004，218(4)：247－256.

[13] Ivanovic, L，Devedzic, G，Cukovic, S，et al．Modeling of the meshing of trochoidal profiles with clearances[J]．Journal of Mechanical Design，2012，134 (4)：041003-1－041003-9.

[14] G. S. Lee，S. Y. Jung，J. H. Bae，et al．Determination of tooth clearances at trochoidal pump[J]．FME Transactions，2011，39 (3)：117－126.

[15] Kwon Soon-man, Kim Chang-Hyun, Shin Joong-ho．Optimal rotor wear design in hypotrochoidal gear pump using genetic algorithm[J]．Journal of Central South University，2011，18(3)：718－725.

[16] Wang ZhenLiu Zhongming. Parameter Design and Anlaysis of Internal Meshing Cyclodial Gear Pump[J].Journal of mechanical transmission,2010，34(2)：35－40.

[17] Xu Yihua，Chen Weiguo，Han Shoulei．Parameter Equation of Cycloid Pump Inner Rotor Theoretic Profile Curve and Modeling of Inner-outer Rotor[J]. Machine Tool & Hydraulics.2008，36(1)：106－107.

[18] Luo Wei-dong，Qiu Wang-biao，Shu Rui-long ,etc．Study Analysis on Interior Tooth of Arc-cycloidal Gear Pump Tooth Shape[J]. Coal Mine Machinetry，2008，29(4)：63－65.

[19] Li Gang．Design Calculation of Cycloid Rotary Pump.Modern Vehicle Power [J]，2007，125(1)：40－42.

[20] Xu Xuezhong. Optimization of the Design Parameters of Cycloidal Pump with Singularity Type Profile[J]．Fluid Machinetry，2005，33(2)：20－23.

[21] Feng Shiyu，Gao Xiufeng,Liu Weihua.Calculation and Analysis on Volume of Working Chambers for Internal-meshing Compressor[J]．China Mechanical Engineering，2008，19(16)：1903－1907.

[22] He Cunxing．Hydraulic Components[M]．Beijing: China Machine Press，1985.（in Chinese）

[23] Yang Guolai,Bai Guixiang,Zhang Shanling．Analysis of Trapping Oil Characteristics of Straight Conjugate Internal Gear Pump[J]. New Technology & New Process，2012，(2)：51－54.

[24] Li Yulong．Mechanism, modeling and experiment Investigation of trapped oil in external gear pump D]．Hefei：Hefei University of Technology，2009．（in Chinese with English abstract）

[25] M Eaton，PS Keogh，KA Edge. The modeling, prediction and experimental evaluation of gear pump meshing pressures with particular reference to aero-engine fuel pumps [J]．Proceedings of the Intitution of Mechanical Engineers Part I-Journal of Systems and Control Engineering，2008，220 (5)：365－379.

[26] Li Yulong，Liu Kun．Dynamic Model of Trapped Oil and Effect of Related Variables on Trapped Oil Pressure in External Spur-gear Pump.[J]．Transactions of the Chinese Society of Agricultural Engineering，2009，40(9)：214－219.

[27] Li Yulong．Summary of Research and Development of Trapped-oil Phenomenon and Trapped- oil Model[J]．Journal of Chengdu University(Natural Science)，2011，30(2)：172－177.

[28] Li Yulong．Establishment and verification of analytic formula for imum trapped-oil pressure in external gear pump[J]．Transactions of the Chinese Society of Agricultural Engineering，2013，29(11)：71－77.

CONFLICT OF INTEREST

We confirm that this article content has no conflict of interest.